

COMPUTATION OF FLOW ABOUT AIRFOILS – COMPARISON OF DIFFERENT METHODOLOGIES

Samuel Víctor S. Maia¹, Luís Morão Cabral Ferro¹

¹*Department of Engineering and Technology, Federal Rural University of Semi-Arid
Avenue Francisco Mota, 572, 59.625-900, RN/Mossoró, Brazil
samuelltivictor_m@hotmail.com, lferro@ufersa.edu.br*

Abstract. The aerodynamic study of an airfoils is fundamental to analyse the behavior and geometrical characteristics of a wing for prescribed flight conditions. Based on analyzes and simulations we are able to define the variables for aerodynamic design of an aircraft. The unmanned aerial vehicle (UAV) designed for SAE Aerodesign competition use high lift profiles for low Reynolds number flow. The viscous or inviscid flow about airfoils can be computed using different methodologies, such as panel method or finite volume method. The main objective of this work is to compute and compare the lift and drag coefficients as well as pressure distributions in the contour of airfoils by calculating the inviscid and viscous flow, using a panel method and a finite volume method. For the analysis, high lift profiles of the families NACA 4, EPPLER, GOE, CH and SELIG were selected. These classes of airfoils have very good aerodynamic efficiency with high ratio between the lift and drag coefficients. These profiles are highlighted by its high mean-line curvature and are used at low speeds, being indicated for the SAE Aerodesign competition aircrafts. The criterion used to choose the airfoil was the highest lift coefficient generated in relation to its maximum stall angle, at a number of Reynolds of cruising flight speed, that is close to the transition from laminar boundary layer to turbulent boundary layer. The panel method analysis was performed using the XFRL5 software that uses XFOIL as source code. In the finite volume method, the Fluent code of ANSYS® was used. Different types of meshes, structured and unstructured, are compared and the quality parameters of the elements generated are analyzed and presented. The pressure distributions and the lift and drag coefficient curves for the selected aerodynamic profile are presented and compared, calculated using the panel method and the finite volume method.

Keywords: Aerodynamic, Aerodesign, Finite volumes

1 Introduction

The aerodynamic characteristics of an airfoil for the wing of an aircraft are strongly important to describe and predict its flight behavior. The computation of aerodynamic coefficients, obtained based on the flow conditions around the surface, are essential for the specification of geometric dimensions and design decisions, of an aircraft destined to participate in the SAE Aerodesign competition.

The lift and the drag are the aerodynamics forces due to the flow about the airfoil. These forces, as well as the pressure distributions on the airfoil contour, can be calculated using numerical methods. According to GUDMUNDSSON [1] the shape of pressure distribution on the contour of the airfoil is very important in the design of the aircraft. The structural loads, the magnitudes of lift, drag and pitch moment, the shock waves and the location of boundary layer transition from the laminar to the turbulent are strongly dependent of pressure distribution on the airfoil contour.

Computer programs that solve potential flows using panel method calculate the velocity distribution on the contour of the profile from the gradient of velocity potential. Panel method codes are a Computer Fluid Dynamics (CFD) alternative of Finite Volume Methods. They are faster and cheaper than Finite Volume Codes and results are reliable when the flow is attached to the airfoils without boundary layer separation. The XFRL5 code was used on the computation of the flow around the airfoil by panel method. This code has good results on the computation of two-dimensional flow at low Reynolds number, as the flow about an airplane model for the SAE competition. The source code of XFRL5 is based on XFOIL code, and, as referred by DRELA [2] the main objective of this code is to reduce compute resources (CPU time) with a good prevision of aerodynamics coefficients for flows with

low Reynolds number, close to the boundary layer transition from laminar to turbulent flow.

The Fluent code of ANSYS® was used to compute the flow by Finite Volume Method (FVM). For viscous flow the $k-\epsilon$ standard model [3] was chosen. Results using different types and configurations (structured and unstructured) meshes are compared. Computed values of lift and drag coefficients for different angles of attack, as well as pressure coefficient distributions on the contour of the airfoil are presented at this paper

The main objective of this paper is to present a comparison of results obtained with the CFD codes, XFLR5 and Fluent, on flow computation about airfoil SELIG 1223 RTL. This airfoil was used in the wing of a model airplane for SAE Aerodesign competition of author's university. Aerodynamic coefficients of lift and drag with angles of attack $\alpha = 0^\circ$, $\alpha = 5^\circ$ and $\alpha = 10^\circ$ computed by panel method and finite volume method with three different meshes, for inviscid and viscous flow, are presented and compared. Distributions of pressure coefficients on the contour of the airfoil, for the same angles of attack are also presented and compared.

2 Aerodynamic forces and pressure distribution

The main components of aerodynamic forces present at an airplane are lift defined by Eq. (1a) and drag by Eq.(1b).

$$L = C_L \frac{1}{2} \rho V_\infty^2 S \quad (1a) \quad D = C_D \frac{1}{2} \rho V_\infty^2 S \quad (1b)$$

where ρ is the density of the air at a specified altitude, V_∞ is the velocity of the airplane (free-stream velocity), S is the planform area of the wing and C_L e C_D are the lift and drag coefficients of the wing, respectively.

These forces are responsible for characterizing the airfoil performance in flight. According to RODRIGUES [4] the lift force represents the highest quality that an aircraft has in comparison to other types of vehicles and defines the ability of an aircraft to remain in flight. Basically, the lift force is used to overcome the weight of the aircraft and thus assure the flight. The lift force (L) has its origin in the pressure difference between the lower and the upper surfaces of an airfoil. In turn the drag force (D) is the resistance of airfoils to the flow. The total drag in the profile is obtained by adding pressure drag and friction drag.

The pressure distribution on the contour of a profile, can be represented using the dimensionless pressure coefficient (C_p), defined by Eq. (2):

$$C_p = \frac{p - p_\infty}{\frac{1}{2} \rho V_\infty^2} \quad (2)$$

where p is the static pressure on the contour of the airfoil and p_∞ is the static pressure at free-stream flow.

3 Airfoil selection

The main characteristics used for airfoil selection were the maximum lift coefficient value and the maximum incidence angle (angle of attack α) in which the stall occurs with the decrease of lift coefficient. In Fig. 1 (a) are shown the evolution of the lift coefficients as a function of the angle of attack for the analyzed profiles, of the NACA, EPPLER, GOE, CH and SELIG families, which are characterized by high lift coefficient and consequently recommended to be used in low speed flow and indicated for aircraft of the type UAV (Unmanned Aerial Vehicle) used in the SAE Aerodesign competition. The geometric characteristics (dimensionless coordinates) of those profiles were get from the digital library of airfoils, developed by the University of Illinois UIUC [5]. The airfoil SELIG 1223 RTL, shown at Fig. 1 (b) has the higher lift coefficient and the higher stall angle between all the analyzed profiles. Airfoil SELIG 1223 RTL was chosen as for simulation with panel and finite volume codes. The main geometric characteristics of selected profile are shown at Fig.1 (b).

Named as *high lift low Reynolds number airfoils* these profiles are used in flows with low Reynolds numbers. They are characterized by a high relative thickness (ratio between the maximum thickness and chord of the profile), by high values of leading edge radius and for having maximum values of relative camber and relative thickness close to the leading edge of the profile. According to ANDERSON [6], the closer to leading edge are the points of maximum relative thickness and camber, bigger are the lift coefficients.

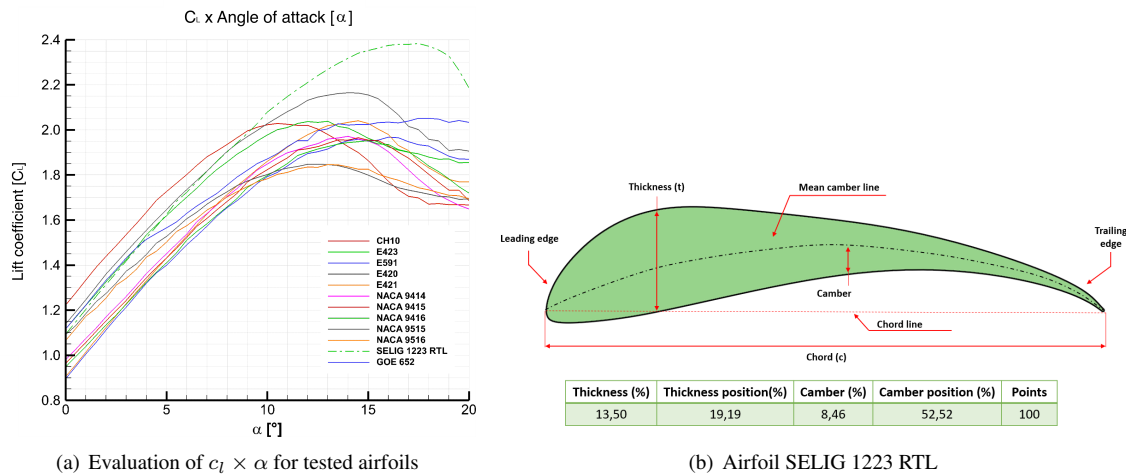


Figure 1. Selection of airfoils: (a) Results of numerical simulation and (b) chosen profile (Author)

4 Panel method

According to ANDERSON [6] for irrotational flows, that is, without presence of vortices, it is possible define a scalar function whose gradient is the flow velocity. When the flow is irrotational a function ϕ , called velocity potential can be defined. This function satisfies the Laplace equation. Thus, Eq. (3) can be written for an incompressible irrotational flow.

$$\nabla \times \vec{V} = \nabla \times \nabla\phi = \nabla^2\phi = 0 \tag{3}$$

A first order panel method is used to compute the flow field. The profile contour and the wake are discretized by straight line segments with a constant source distributions σ on each panel. The intensity of the vortex distribution varies linearly on the profile contour and has a constant value on the wake. In the chosen panel code, a stream function Ψ formulation is used. The stream function Ψ is defined by Eq. (4) in DRELA [7], where u_∞ is free-stream velocity component in the x direction and v_∞ is the component in the y direction, s is the coordinate along the vortex and source sheets, r is the magnitude of the vector between the point at s and the field point x, y , and θ is the vector angle.

$$\Psi(x, y) = u_\infty y - v_\infty x + \frac{1}{2\pi} \int \gamma(s) \cdot \ln r(s; x, y) ds + \frac{1}{2\pi} \int \sigma(s) \cdot \theta(s; x, y) ds \tag{4}$$

At the inviscid formulation, the vortex distribution is computed imposing that the profile contour is a stream-line. The stream function Ψ has a constant value on the contour profile and the source distribution has zero intensity. For the viscous formulation the value of the source distribution is obtained from the solution of the boundary layer integral equation boundary and represented by a transpiration speed in the profile contour. The final velocity field is obtained solving systems of non-linear equations using Newton's method.

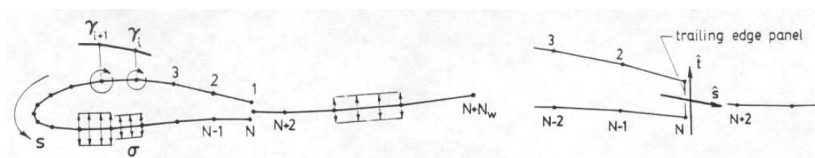


Figure 2. Vortex distribution and panel discretization of the airfoil (DRELA, 1989)

$$L' = \rho_\infty V_\infty \int \gamma ds \tag{5}$$

4.1 Simulation with XFLR5/XFOIL

The contour of the airfoils was discretized in one hundred panels. This discretization was considered enough to allow a better convergence of results at certain angles of attack α . At the midpoint of each panel there is a

control point where the boundary conditions were prescribed and the velocities calculated, as well as the pressure coefficients.

Taking account the altitude and local conditions present at the place where the SAE Aerodesign competition occurs and for a cruise velocity (free-stream velocity) of the airplane equal to 16 m/s the Reynolds number, was calculated by Eq. (6a), where ρ_∞ is the density of the air, V_∞ the free-stream flow velocity, c the airfoil chord and μ the dynamic viscosity of the air. The Mach number, Ma , of the flow can be calculated from Eq. (6b), where U_∞ is the average speed of sound. The dimensionless values obtained were $Re = 4.89 \times 10^5$ and $Ma = 0.047$.

$$Re = \frac{\rho_\infty V_\infty c}{\mu} \quad (6a) \qquad Ma = \frac{V_\infty}{U_\infty} \quad (6b)$$

The lift and drag coefficients, c_l and c_d , for a Reynolds number $Re = 4.89 \times 10^5$ and Mach number, $Ma = 0.047$, were computed for angles of attack from $\alpha = 0^\circ$ to $\alpha = 20^\circ$, for inviscid and viscous flows. The computed values for $\alpha = 0^\circ$, $\alpha = 5^\circ$ and $\alpha = 10^\circ$ are presented and compared at Tab. 1.

Table 1. Lift and drag coefficients, computed by XFLR5, for inviscid and viscous flows

Angle of attack (α)	c_l (Visc.)	c_l (Invisc.)	c_d (Visc.)
0°	1.1032	1.5295	0.0151
5°	1.6324	2.1192	0.0196
10°	2.0742	2.6925	0.0274

5 Finite Volume Method

The finite volume method code FLUENT of ANSYS® was used to compute both inviscid and viscous flows about the airfoils. The computational domain used, as well as, mesh discretization of domain, boundary conditions applied and main results for the flow about airfoil SELIG 1223 RT are presented as follow.

5.1 Definition of computational domain and boundary conditions

The maximum dimensions of the domain were defined in order to reduce the interference in the flow around the airfoil. The input section of the control volume is a semicircle with a radius equal to ten times the chord length and the center on the leading edge. The boundary condition prescribed at this region is *velocity inlet*. The prescribed value is equal to free-stream velocity.

The outlet section of the domain is placed ten chords downstream of the trailing edge of the profile. A pressure boundary condition is used at this section (*pressure-outlet*). Pressure at outlet section will be extrapolated from the flow in the interior of the domain.

The third contour region are the side walls of the domain. The boundary condition used is the pressure far field boundary condition (*pressure-far-field*). According to ANSYS [8] this configuration is used to model a free stream condition at infinity based on the Mach number and the specified static pressure conditions.

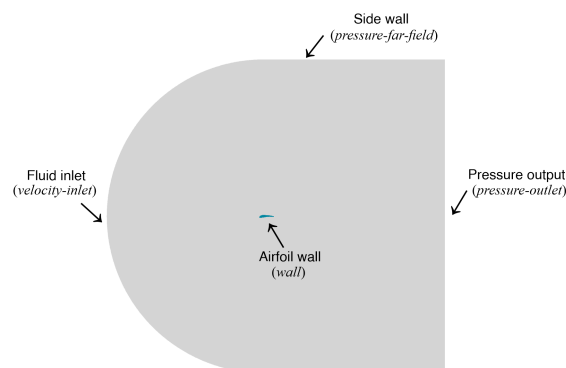


Figure 3. Simulation domain (Author)

5.2 Mesh configurations

Figure 4 shows the three meshes used on the discretization of the computational domain. The mesh (a) is structured with quadrilateral elements and the mesh (b) unstructured with triangular elements. Meshes (a) and (b) were designed with *Mesh* code from ANSYS. Mesh (c), also shown at Fig. 4, was designed using ICEM CFD code. This mesh is structured with quadrilateral elements, and a refined zone at the wake flow and an *inflation* procedure from the airfoil contour to the external boundary, with a total discretization of the domain. The smaller mesh elements are close to the airfoil contour.

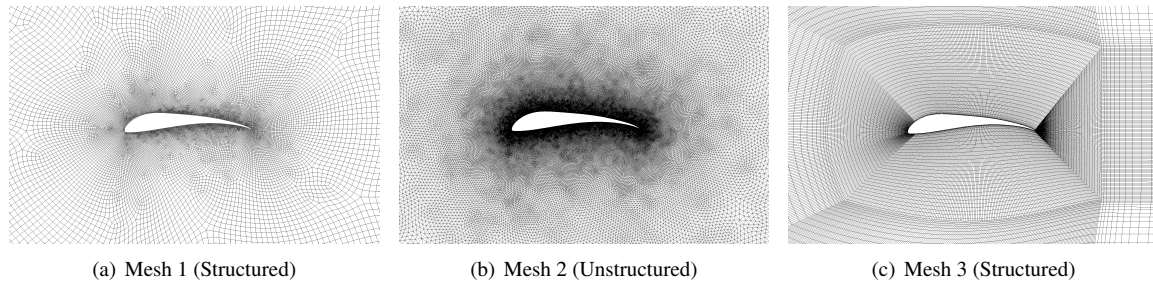


Figure 4. Meshes configuration close to the airfoils : (a) quadrilateral, (b) triangular e (c) quadrilateral (Author)

Although meshes (a) and (b) (Fig 4) almost has the same number of mesh nodes, the unstructured mesh (b) has a smaller number of elements. Also the unstructured mesh has more elements close to the airfoil contour than the structured mesh. Unstructured mesh needs yet less number of elements than structured mesh to discretize with quality curve regions close the airfoil. Structured meshes also have a longer processing time (CPU time) in their generation than unstructured meshes. The data regarding the number of nodes and elements for the meshes shown in the Fig 4 are presented at Tab. 2.

5.3 Quality parameters of computational meshes

The mesh values of quality statistics parameters were obtained by ANSYS® Grid. Using the *quality* option, the parameters *skewness*, *orthogonal quality* and *element quality* were evaluated. In Tab. 2 the values of those parameters for the three meshes are presented. The values of quality parameters vary on a range between zero and one.

Table 2. Quality and statics parameters of computational meshes

Skewness					
Mesh number	Elements average	Standard Deviation	Quality of elements	Number of nodes	Number of elements
1	0.1359	0.0997	Excellent	133264	132284
2	0.0497	0.0496	Excellent	127022	251952
3	0.2430	0.1759	Excellent	142404	141560
Orthogonal quality					
1	0.9689	0.0389	Excellent	-	-
2	0.9694	0.0306	Excellent	-	-
3	0.9414	0.0495	Excellent	-	-
Element quality					
1	0.8737	0.0936	-	-	-
2	0.9668	0.0326	-	-	-
3	0.9540	0.0430	-	-	-

The *skewness* is on of the primary quality parameters of a mesh and shows the asymmetry of the elements generated from the mesh. The lower this value, the less the mesh will be distorted from a standard element. The skewness value for an equilateral element is zero.

The parameter *orthogonal quality* is a measure of how close the angles of adjacent element edges are to optimal angle. For the unstructured mesh, the triangular elements are considered perfect when the triangles are

equilateral. For the structured mesh, the better the quadrilateral elements are rectangles. The value of orthogonal quality parameter for rectangles and equilateral triangles is one. For a range between 0.95 and 1.00 the mesh is excellent ANSYS [9].

The parameter *element quality* show the quality of mesh elements relative to its distribution on the domain or mesh. This parameter is defined by Eq. 7.

$$Quality = C \frac{S_e}{\sum L^2} \quad (7)$$

where S_e is the element area, L the edge length and C is a dimensionless constant, with $C = 6.92820323$ for triangle elements and $C = 4.0$ for quadrangle elements (ANSYS [8]). According to [10] a value of 1 indicates a perfect cube or square while a value of 0 indicates that the element has a zero or negative volume.

5.4 Simulation with Fluent

The computed results for lift and drag coefficients, obtained with the three referred meshes, for the angles of attack $\alpha = 0^\circ$, $\alpha = 5^\circ$ and $\alpha = 10^\circ$ are presented at Tab.3.

Table 3. Results computed by Fluent

Angle of attack α	Mesh 1			Mesh 2			Mesh 3	
	c_l (Visc.)	c_l (Invisc.)	c_d (Visc.)	c_l (Visc.)	c_l (Invisc.)	c_d (Visc.)	c_l (Visc.)	c_d (Visc.)
0°	1.1777	1.5905	0.0231	1.0451	1.5128	0.0210	1.0792	0.0591
5°	1.6926	2.1910	0.0314	1.5655	2.1223	0.0287	1.6393	0.0825
10°	2.0921	2.8332	0.049	2.0635	2.8187	0.0478	2.0313	0.1291

A good agreement of inviscid lift coefficients of mesh 2 is observed with those obtained for mesh 1, with a relative difference smaller than 5%. The values of the lift and drag coefficients on mesh 1 and 2 do not have such a good agreement on viscous flow. These values depend on mesh topology and discretization and mesh type configuration in the nearby elements of the profile, boundary layer region. On boundary layer region a more refined mesh is needed to capture the viscous effects generated by the flow. A third mesh configuration was then used to improve the results for drag and lift coefficients and to preview the stall angle with accuracy. This last mesh (mesh 3) is structured, with a boundary layer mesh and inflation. The inflation factor depends on the thickness of the smaller element close to the airfoil and the total number of elements on the mesh.

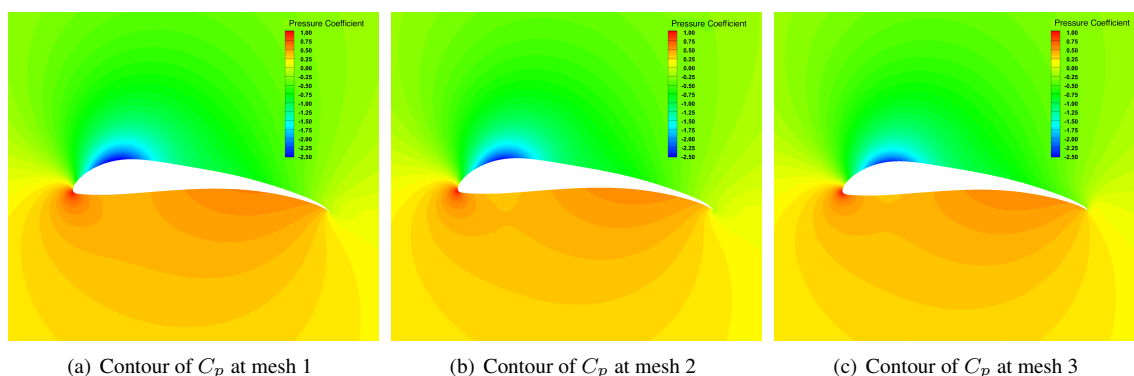


Figure 5. Pressure coefficient distributions at meshes 1, 2 and 3 for $\alpha = 5^\circ$ (Author)

In Fig. 6 pressure distributions calculated by panel method and finite volume method with the code FLUENT, for viscous flow with an angle of attack $\alpha = 5^\circ$, are compared. The two methods show a good agreement between the results computed by panel method and finite volume method. The small difference between the lift results 6(a) and the pressure coefficient distribution 6(b) can be associated with the type of mesh used, as the solver works with a system of solutions of equations for each mesh node. Another factor that may have affected the results is the interference generated by the domain itself and its boundary conditions applied. Even so, the presented values have a good reliability and can be used later to compare results obtained through different meshing methodologies and simulation methods.

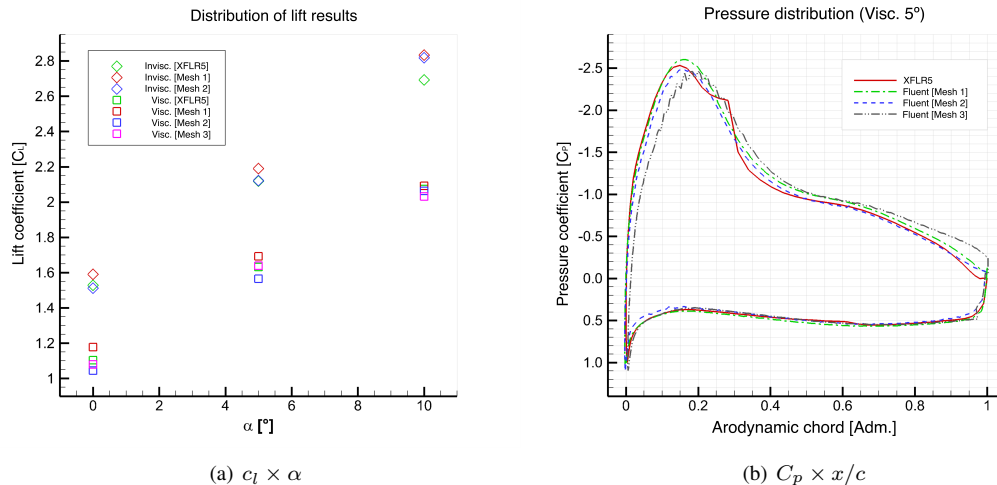


Figure 6. Comparison of $c_l \times \alpha$ and $C_p \times x/c$ evolutions for $\alpha = 5^\circ$ computed by XFLR5 and by Fluent. (Author)

6 Conclusion

A comparison of panel method and finite volume method on the computation of the inviscid and viscous flow about airfoil SELIG 1223 RTL was presented. The panel method code was XFLR5 and the finite volume code the Fluent from ANSYS. At Fluent code the turbulence for viscous flow computation was modelled by $k - \epsilon$ standard model. On the computation by Fluent the domain was discretized by three different meshes: a structured mesh, an unstructured mesh and a structured mesh with boundary layer. It was verified that the reliability of the results depends on the quality of the generated mesh as well as the type of solution applied for the viscous analysis.

For the three types of mesh and for the $k - \epsilon$ standard turbulence model the third topology has a more uniform behavior with results closer to the values computed by XFLR5. Another way to carry out the comparative study for the three meshes would be through a later analysis, carrying out simulations using other turbulence models available on Fluent code, and through this make a balance of the new computed results and comparing with the values present in this article.

Acknowledgment

The work presented in this article was financially supported by Extension and Culture Dean of the Federal Rural University of Semi-Arid through the Engineering: Utility and Applicability (Engenharia: Utilidade e Aplicabilidade) program.

References

- [1] GUDMUNDSSON, S., 2014. *General Aviation Aircraft Design: Applied Methods and Procedures*. The Boulevard, Langford Lane, Kidlington, Oxford OX5 1GB, UK.
- [2] DRELA, M., 2000. *Xfoil*. <https://web.mit.edu/drela/Public/web/xfoil/>. Acesso em: 15 Nov. 2019.
- [3] LAUDER, B. E. & SPALDING, D., 1972. *Lectures in Mathematical Models of Turbulence*. Academic Press, New York.
- [4] RODRIGUES, L. E. M. J., 2013. *Fundamentos da engenharia aeronáutica*. São Paulo: Cengage Learning.
- [5] UIUC, Procurar ano. *Department of Aeronautical and Astronautical*. <https://m-selig.ae.illinois.edu/ads.html>. Acesso em: 22 Nov. 2019.
- [6] ANDERSON, J., 2010. *Fundamentals of Aerodynamics*. Nova York: McGraw-Hill Book Company.
- [7] DRELA, M., 1989. An analysis and design system for low reynolds number airfoils. In *Low Reynolds number aerodynamics*, pp. 1–12, Springer, Berlin, Heidelberg.
- [8] ANSYS, 2013. *ANSYS Fluent User's Guide*. ANSYS, Inc, Southpointe, 275 Technology Drive, Canonsburg, PA 15317.
- [9] ANSYS, 2009. Appendix A - mesh quality. ANSYS Meshing Application Introduction. <http://dl.mr-cfd.com/tutorials/meshing/ansys-meshing/mesh-quality-ansys-meshing.ppt>, Last accessed on 2020-14-10.
- [10] ANSYS, 2010. *ANSYS Mesh User's Guide*. ANSYS, Inc, Southpointe, 275 Technology Drive, Canonsburg, PA 15317.